Modeling and Optimization of Polyester Polymerized Esterification Process

Xiuli Zhu[1,3], Kuangrong Hao[1,3*], Biao Huang[2,4*], Yicun Hua[1,3], Lei Chen[1,3], Xin Cai[1,3]

1 College of Information Sciences and Technology, 2 College of Chemical and Materials Engineering,

3 Engineering Research Center of Digitized Textile &Apparel Technology, Ministry of Education, Donghua University, Shanghai 201620, China

4 University of Alberta, Edmonton, Alberta, T6G2V4, Canada

Correspondence to: Kuangrong Hao (krhao@dhu.edu.cn), Biao Huang (biao.huang@uablerta.ca)

***Abstract*—The esterification in polymerization process is the most important step in polyester fiber production. In this paper, first, a new first-principle model is built by including extra formation of acetaldehyde, which has been largely neglected in the literature. Second, there exist four objectives to optimize in the process of esterification, including rate of esterification, average molecular weight, degree of polymerization and diethylene glycol content percentage. However, most researchers have considered only one or two of the four performance indicators which may not completely reflect the actual state of PET polymerization process. In this work, an improved RVEA algorithm, called PARVEA, is proposed to deal with a four-objective optimization problem combining with a new first-principle model in esterification process. Then, PARVEA is further compared with other four algorithms on the test problems of seven widely used benchmarks, and the four-objective optimization problem in esterification process. Experimental results indicate that PARVEA not only outperforms the four algorithms in terms of both IGD and HV metrics, but also optimizes the esterification process. Finally, companies can choose more suitable solutions and process parameters according to user preferences, which can meet the requirements for differentiated production of high-quality polyester fiber polymers.**

***Index Terms*—Multi-objective evolutionary algorithm, Polyester, Esterification process, RVEA**

I. Introduction

Polyester is the raw material for manufacturing polyester fiber, coating, film and engineering plastics[1]. Polyester is also called terri black silk ribbon. Polyester fiber production process mainly consists of three stages, which are accordingly polymerization process, melt transport process and spinning process. The polymerization process plays an important role in polyester fiber

production. It is composed of three stages, namely, esterification process, pre-condensation stage and final-condensation stage[2].

The esterification process is mainly determined by four physical properties of the material, including the rate of esterification, the percentage of diethylene glycol, the degree of polymerization and the average molecular weight[3].It is commonly known that the average molecular weight of polymer determines several important physical properties of the material[4-6], such as strength and impact resistance. The content of diethylene glycol in polyester chips is a strictly controlled index. In theory, due to the existence of diethylene glycol, the ether bond in diethylene glycol when being added to the polyester macromolecular segment, will destroy the polymer to a certain extent. The regularity of the arrangement of the ester macromolecular chains reduces the strength of the chains. In addition, the increase of diethylene glycol content also slightly reduces the melting point of the slices. All aspects have caused the reduction of the fiber-forming performance of the chip. As a result, a high rate of broken heads will occur which leads to a poor quality of polymer product[7].

Because the esterification reaction is a solid phase, liquid phase and gas phase naphthalene system, the actual reflection system is more complicated. Liu[8] *et al*. built the mathematical model of esterification reactor and gave the model parameters. Wu[9] *et al*. built the direct esterification model of polyester based on the reaction mechanism of polyester esterification and the actual process conditions. However, this paper only considers some of the chemical reactions that generate by-products acetaldehyde. The production of acetaldehyde will affect the quality of the polymer, so in the production process of polyester fibers, we want to minimize the generation of acetaldehyde[10].

Meanwhile, almost all the formation of diethylene glycol occurs in the esterification stage. The content of terminal carboxyl group in the pre-condensation stage is closely related to the esterification rate of the esterification reaction. Therefore, the optimization of esterification process is of great importance[11].

With increase of temperature, pressure, radio of slurry and resident time, the percentage of diethylene glycol is increased which will result in failure of products to meet the quality specifications. Thus, among the four performance indexes in esterification process, we want to maximize the rate of esterification, the degree of polymerization and the average molecular weight while minimizing the percentage of diethylene glycol. In summary, among the four objectives for optimization of esterification process, there is a conflict[12].

The average molecular mass M_n, the degree of polymerization P_n, the esterification rate E_s and the percentage of diethylene glycol W_t play equally important roles in the process of polyester fiber polymerization esterification for production. Therefore, taking account of additional factors from the actual esterification process is necessary, and implementing high-dimensional multi-objective optimization of esterification process is imperative[13].

With the development of multi-objective evolutionary algorithms (MOEA), it is possible to consider multiple objectives at once without significantly increasing computation time in industrial process[14-19]. For this reason, multi-objective EAs (MOEAs) have

been well developed since the past two decades. Generally, these algorithms can be classified into two categories.

The first category includes the Pareto dominance method combined with preference information. The second category is the algorithm based on decomposition, which decomposes an MOP into several sub-problems, and the best candidate of each sub-problem forms the final solution set. For example, a multi-objective evolutionary algorithm based on decomposition (MOEA/D)[20]decomposes an MOP into a number of sub-problems using a set of predefined reference vectors and optimizes the sub-problems simultaneously. Then a reference vector guided evolutionary algorithm (RVEA) is proposed by Cheng[21] *et al.* RVEA is superior to other algorithms when solving the multi-objective optimization problems in a high-dimensional space. Because the angle-penalized distance (APD) is introduced to balance not only diversity but also convergence with adaptive reference vectors.

Nevertheless, RVEA has some deficiencies in dealing with the multi-objective optimization of the esterification process. For example, RVEA cannot update the weight vector in real time according to the distribution of solutions[21].

The main contributions of this paper are as follows:

①An improved first principle model of esterification stage is developed which incorporates the extra reaction of acetaldehyde. Through considering more comprehensive chemical side reactions, we will simulate the actual polymerization and esterification process better, thereby minimizing the content of diethylene glycol as a side reaction product, and effectively improving product quality;

②A four-objective optimization method PARVEA in esterification process is proposed based on the improved RVEA algorithm;

③The distribution between the upper and lower solutions is compared, and then the reference vector is updated adaptively by using Pearson correlation coefficient in PARVEA algorithm;

④ The formula of particle environment selection based on Angle-Penalized Distance (APD) is improved to accelerate the population convergence by introducing projection distance;

⑤ PARVEA is compared with other four algorithms on seven widely used benchmark test problems and the four-objective optimization problem in esterification process.

The rest of this paper is organized as follows: Section II briefly presents the improved first-principle model and the four-objective optimization problem of esterification process. Section III presents reference vector guided evolutionary algorithm and its improvement PARVEA. Section IV optimizes the four-objective esterification process and compares effectiveness with other four algorithms on seven widely used benchmark test problems by PARVEA. Finally, conclusions and future work are presented in Section V.

II. Problem Description

A. *Improved First principle Model of Esterification Process*

Commercially, the polymerization process of PET consists of three stages using continuous reactors. These are esterification stage, pre-condensation stage and final-condensation stage, respectively. The raw materials commonly used are one molar excess of ethylene glycol (EG) and either purified terephthalic acid (PTA) or dimethyl terephthalate (DMT) with ethylene glycol antimony as catalyst.

Our study is based on the current popular PTA route. The process involves mixing terephthalic acid with ethylene glycol in a certain proportion in the slurry tank, and then the prepared slurry is pumped to the buffer tank and continuously sent into the esterification reactor. The esterification process is then carried out under certain pressure, temperature and material self-circulation. Then the product is sent to pre-polycondensation reactor. Finally, the high polymer enters the final polycondensation reactor and completes the formation of the final polymer through mass transfer. Each polycondensation reactor unit is equipped with an ethylene glycol spray condensation system for absorption of ethylene glycol from the condensation reaction, and also equipped with a vacuum generation system (vacuum pump) to provide vacuum power for the condensation reaction[22].The polymerization process is shown in Fig.1.

Esterification process is the first and most important stage of polymerization process. The process of polyester esterification includes esterification reaction apparatus and process tower, etc. EG and PTA are pre-mixed in the mixing tank and pumped into the esterification reactor. The gas phase in the esterification reactor mainly consists of ethylene glycol and water. After separating from the process tower connected to the esterification reactor, the liquid phase mixture containing 95% ethylene glycol and 5% water in the process tower kettle is returned to the esterification reactor, and the products containing most of the water on the top of

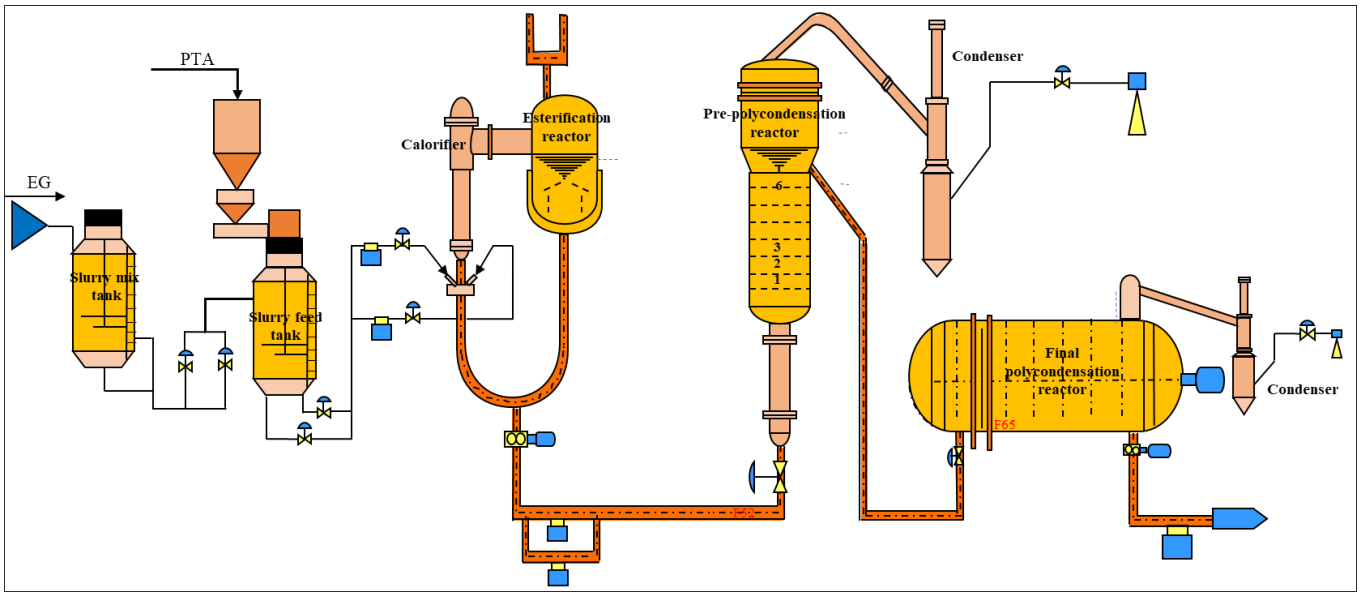

Fig.1. Polymerization process

TABLE I.

Kinetic scheme and kinetic parameters

Kinetic Scheme

(1) Ester interchange reaction (main polycondensation) ($\mathbb{F}$ replaces benzene ring)

$$\sim \mathbb{F} \sim \underset{c_1}{COOH} + \underset{c_2}{C_2H_4(OH)_2} \overset{k_1/k_2}{\rightleftarrows} \sim \mathbb{F} \sim \underset{c_3}{COO(CH_2)_2OH} + \underset{c_5}{H_2O}$$

$$\sim \mathbb{F} \sim \underset{c_1}{COOH} + \underset{c_3}{HO(CH_2)_2OOC} \sim \mathbb{F} \sim \overset{k_3/k_4}{\rightleftarrows} \sim \mathbb{F} \sim \underset{c_4}{COO(CH_2)_2OOC} \sim \mathbb{F} \sim + \underset{c_5}{H_2O}$$

(2) Poly-merization recation

$$2(\sim \mathbb{F} \sim \underset{c_3}{COO(CH_2)_2OH}) \overset{k_5/k_6}{\rightleftarrows} \sim \mathbb{F} \sim \underset{c_4}{COO(CH_2)_2OOC} \sim \mathbb{F} + \underset{c_2}{C_2H_4(OH)_2}$$

(3)Diethylene glycol side reaction

$$2(\sim \mathbb{F} \sim \underset{c_3}{COO(CH_2)_2OH}) \xrightarrow{k_7} \sim \mathbb{F} \sim \underset{c_6}{COO(CH_2)_2O(CH_2)_2OOC} \sim \mathbb{F} \sim + \underset{c_5}{H_2O}$$

$$(\sim \mathbb{F} \sim \underset{c_3}{COO(CH_2)_2OH}) + \underset{c_2}{C_2H_4(OH)_2} \xrightarrow{k_8} \sim \mathbb{F} \sim \underset{c_7}{COO(CH_2)_2O(CH_2)_2OH} + \underset{c_5}{H_2O}$$

$$\underset{c_2}{2C_2H_4(OH)_2} \xrightarrow{k_9} \underset{c_8}{HO(CH_2)_2O(CH_2)_2OH} + \underset{c_5}{H_2O}$$

$$\sim \mathbb{F} \sim \underset{c_1}{COOH} + \underset{c_8}{HO(CH_2)_2O(CH_2)_2OH} \overset{k_1/k_2}{\rightleftarrows} \sim \mathbb{F} \sim \underset{c_7}{COO(CH_2)_2O(CH_2)_2OH} + \underset{c_5}{H_2O}$$

(4)Acetaldehyde side reaction

$$\sim \mathbb{F} \sim \underset{c_3}{COO(CH_2)_2OH} \xrightarrow{k_{10}} \sim \mathbb{F} \sim \underset{c_1}{COOH} + \underset{c_9}{CH_3CHO}$$

Kinetic parameters in esterification reaction T=536.15K

	A_i	E_i	k_i
1	1.80E+09	19640	17.73934
2	1.85E+08	18140	7.435587
3	4.57E+09	22310	3.673931
4	7.98E+07	18380	2.56604
5	9.09E+00	2810	0.650474
6	6.82E+06	14960	5.436844
7	2.49E+15	42520	0.011548
8			0.023096
9			0.046192
10	8.32E+7	117982	6.66E-41

the process tower are further processed in other equipment. During the esterification process of PTA and EG, water is continuously released, and the system is transformed from heterogeneous phase to homogeneous phase, and from turbidity transparency to the point of clarity. In the process of transition from esterification to polycondensation, the system gradually thickens and breaks out EG, finally producing a high viscosity PET melt[23-24].

TABLE II
The first principle model of esterification process

Balance equations for the liquid phase

$$\frac{dc_1}{dz} = \frac{(F_0 b_{10} - F c_1)}{W} + R_1$$

$$\frac{dc_2}{dz} = \frac{(F_0 b_{20} - F c_2)}{W} + R_2 - \frac{Q_{EG} h_{EG}}{W} + \frac{q_{EG} h_{EG}}{W}$$

$$\frac{dc_3}{dz} = \frac{(F_0 b_{30} - F c_3)}{W} + R_3$$

$$\frac{dc_4}{dz} = \frac{(F_0 b_{40} - F c_4)}{W} + R_4$$

$$\frac{dc_5}{dz} = \frac{(F_0 b_{50} - F c_5)}{W} + R_5 - \frac{Q_{H_2O} h_{H_2O}}{W}$$

$$\frac{dc_6}{dz} = \frac{(F_0 b_{60} - F c_6)}{W} + R_6$$

$$\frac{dc_7}{dz} = \frac{(F_0 b_{70} - F c_7)}{W} + R_7$$

$$\frac{dc_8}{dz} = \frac{(F_0 b_{80} - F c_8)}{W} + R_8$$

$$\frac{dc_9}{dz} = \frac{(F_0 b_{90} - F c_9)}{W} + R_9$$

$$\frac{dc_{10}}{dz} = \frac{(F_0 b_{100} - F c_{10})}{W} + R_{10}$$

$$R_1 = -k_1 c_1 c_2 + k_2 c_3 c_5 - k_3 c_1 c_3 + k_4 c_4 c_5 - k_1 c_1 c_8 + k_2 c_5 c_7 + k_{10} c_3$$

$$R_2 = -k_1 c_1 c_2 + k_2 c_3 c_5 + k_5 {c_3}^2 - k_6 c_2 c_4 - k_8 c_2 c_3 - 2k_9 {c_2}^2$$

$$R_3 = k_1 c_1 c_2 - k_2 c_3 c_5 - 2k_5 {c_3}^2 - k_3 c_1 c_3 + k_4 c_4 c_5 + k_6 c_2 c_4 - 2k_7 {c_3}^2 - k_8 c_2 c_3 - k_{10} c_3 - k_5 c_{10} c_3$$

$$R_4 = k_3 c_1 c_3 - k_4 c_4 c_5 + k_5 {c_3}^2 - k_6 c_2 c_4 + k_5 c_{10} c_3$$

$$R_5 = k_1 c_1 c_2 - k_2 c_3 c_5 + k_3 c_1 c_3 - k_4 c_4 c_5 + k_7 {c_3}^2 + k_8 c_2 c_3 + k_9 {c_2}^2 + k_1 c_1 c_8 - k_2 c_5 c_7$$

$$R_6 = k_7 {c_3}^2$$

$$R_7 = k_8 c_2 c_3 + k_1 c_1 c_8 - k_2 c_5 c_7$$

$$R_8 = k_9 {c_2}^2 - k_1 c_1 c_8 + k_2 c_5 c_7$$

$$R_9 = k_{10} c_3 + k_5 c_{10} c_3$$

$$R_{10} = -k_5 c_{10} c_3$$

Gas-liquid equilibrium equation

$$x_{EG} r_{EG} P_{EG}^s = P y_{EG}$$

$$x_{H_2O}\, r_{H_2O} P_{H_2O}^s = P y_{H_2O}$$

$$Q_{EG} = K_{EG} \alpha (P_{EG}^s - P y_{EG})$$

$$q_{EG} = Q_{EG} - Q_{H_2O} * 0.004$$

$$Q_{H_2O} = K_{H_2O} \alpha (P_{H_2O}^s - P y_{H_2O})$$

$$k_i = A_i * exp\left(\frac{-E_i}{R * T}\right)$$

$$log\, P_{EG}^s = 7.8808 - 1957/(T + 193.8)$$

$$log\, P_{H_2O}^s = 7.9668 - 1668.2/(T + 228)$$

The first stage takes place in an esterification reactor, where various reactions occurring are given in TABLE I in [3]. However, from [5], it can be seen that the formation of side reactions to acetaldehyde is more than one. Specifically, there is extra reaction shown as follows in Eq (1).

$$\sim \mathbb{F} \sim \underset{c_{10}}{COOCH} = CH_2 + \sim \mathbb{F} \sim \underset{c_3}{COO(CH_2)_2OH} \xrightarrow{k_5} \sim \mathbb{F} \sim \underset{c_4}{COO(CH_2)_2OOC} \sim \mathbb{F} \sim + \underset{c_9}{CH_3CHO} \quad (1)$$

Thus, the first-principle model of esterification process has been improved by adding Eq. (2).

$$\frac{dc_{10}}{dz} = \frac{(F_0\, b_{100} - Fc_{10})}{W} + R_{10} \quad (2)$$

The first principle model for the present study is based on the general step-growth polymerization kinetic scheme with some reasonable assumptions[3] shown in TABLE II, where c_i represents the concentration of component i with the unit mol/kg. Specifically, c_1 represents carboxyl-terminated (terephthalic acid), c_2 represents ethylene glycol, c_3 is hydroxyl terminated (dihydroxyethyl terephthalate), c_4 is ester group (PET polymer), c_5 represents the water, c_6, c_7 and c_8 represent various forms of diethylene glycol respectively, c_9 represents the acetaldehyde, and c_{10} represents polymer formed in the esterification process. Similarly, $b_{10} - b_{100}$ represent the initial concentration from component c_1 to c_{10} respectively, $k_1 \sim k_{10}$ represent chemical reaction rate constants with units of $k_1 \sim k_9$ and k_{10} being $mol/kg \cdot h$ and 1/h, respectively. Scalar z varies from 0 to 1. T is the temperature of esterification process. W is the total mass of the reaction mixture in the reactor with unit kg, F_0 is the incoming flow with unit kg/h, F is the outgoing flow with unit kg/h. P_{EG}^s and $P_{H_2O}^s$ are the saturated vapor pressure of EG and H_2O with unit $mmHg$ respectively. h_{EG} and h_{H_2O} represent equilibrium concentration of EG and H_2O respectively. Q_{EG} and Q_{H_2O} represent the amount of ethylene glycol transferred from the liquid phase to the gas phase, that is, the evaporation of EG in the reactor, and the amount of water transferred from the liquid phase to the gas phase, that is, the evaporation of water in the reactor. q_{EG} is the flow rate of EG from the separation tower back to the reactor with unit kg/h. $K_{EG}\alpha, K_{H_2O}\alpha$ are the mass transfer coefficient of EG and H_2O respectively. A_i is the frequency factor. E_i is the reaction activation energy in units of cal/mol. R is the gas constant in unit of $cal/(mol * K)$. Last, y_{EG} and y_{H_2O} are the gas phase molar fraction of EG and H_2O respectively, x_{EG} and x_{H_2O} are the liquid phase molar fraction of EG and H_2O, and P is the total pressure in the reactor with unit $mmHg$. Various parameters take values consistent with values of [5] in this paper.

B. Four-objective Optimization of Esterification Process

The improved first principle model of esterification process is shown in TABLE II.

The esterification rate E_s(the unit is %):

$$E_s = (b_{10} - c_1)/b_{10} \quad (3)$$

The percentage of diethylene glycol W_t(the unit is %):

$$W_t = (c_{DEG} * W_{DEG})/1000 * 100\% \quad (4)$$

The average molecular mass M_n (the unit is 1):

$$M_n = 2000/(c_1 + c_3 + c_8) \quad (5)$$

The degree of polymerization P_n (the unit is 1):

$$P_n = \left(M_n + 26.03 + b_{100} - 88.1 \times (c_3 - b_{30})/(b_{10} + b_{30})\right)/192.17 \quad (6)$$

As mentioned, b_{100} , b_{30} and b_{10} represent the initial concentrations of three components shown in TABLE I respectively. W_{DEG} represents the mass of diethylene glycol. Similarly, c_{DEG} represents the concentration of diethylene glycol.

To the best of our knowledge, the higher the esterification rate E_s, the average molecular weight M_n and the degree of polymerization P_n, the lower the percentage of by-product diethylene glycol W_t, quality and performance of the polymer during the esterification stage will be better.

Expressed mathematically, this optimization problem can be written as:

$$\text{Minimize} \quad J_1 = W_t \quad (7)$$

$$\text{Maximize} \quad J_2 = E_s \quad (8)$$

$$J_3 = M_n \quad (9)$$

$$J_4 = P_n \quad (10)$$

TABLE III
Effect of an increase in the decision variable (DV) on the objective functions

Objective function	Effect of increase in DV			
	T	P	τ	r
M_n	↑↓	↑↓	↑↓	↑↓
E_s	↑↓	↑↓	↑↓	↑↓
P_n	↑↓	↑↓	↑↓	↑↓
W_t	↑	↑	↑	↑

As shown in TABLE III, we can conclude that with the increase of reaction conditions within a reasonable range M_n , E_s, P_n and W_t will increase. However, as seen from Eq. (7)-Eq. (10), we want to maximize M_n , E_s, P_n while minimizing W_t. Thus, there are conflicts among the effects of the decision variables in the four objective functions. As a result, the optimum will be a Pareto-optimal set rather than a single optimum. Furthermore, since optimization algorithms usually deal with either the maximization or minimization problem, a four-objective function is then formulated through the following minimization problem:

$$min\, I\,(T, P, \tau, r) = [1/M_n, 1/P_n, 1/\,E_s, W_t]^T \quad (11)$$

Where T, P, τ, r represent four different decision variables. They represent the temperature, pressure, the ratio of slurry and the residence time of esterification process respectively. $1/M_n, 1/P_n, 1/\,E_s, W_t$ are different objective functions.

The following bounds are used for the decision variables based on industrial requirements:

$$270 \leq T \leq 290\ ^0C \quad (12)$$

$$755 \leq P \leq 770 mmHg \quad (13)$$

$$1.1 \leq \mathrm{r} \leq 1.4 \qquad (14)$$

The residence time is not disclosed in this article for proprietary reasons. Meaningful bounds have been chosen on the four decision variables u based on industrial requirements.

III. Reference Vector Guided Evolutionary Algorithm and Its Improvement

A. *Definition of Multi-objective Optimization*

Multi-objective optimization problems (MOPs), can be mathematically formulated as follows:

$$\begin{aligned} &min\ F(x) = \left(f_1(x), f_2(x), \ldots, f_m(x)\right)^T \\ &subject\ to\ g_i(x) \leq 0, i = 1, \ldots p \qquad (15) \\ &h_j(x) = 0, j = 1, \ldots q \\ &x \in \Omega_x \end{aligned}$$

where $x = (x_1, x_2, \ldots x_n)^T \in X \subset R^n$ are decision variables in the search space X of n dimensions. $F = (f_1, f_2, \ldots, f_m)^T$ is m-dimension target space of objective vectors. $g_i(x) \leq 0$and $h_j(x) = 0$ are ith inequality constraint and jth equality constraint, respectively. p represents the number of inequality constraints; q represents the number of equality constraints.

In multi-objective optimization, just as its name implies, there are several objectives to be optimized. Commonly, it has two conditions. First, the optimization consists of conflicting objectives. Second, a solution set that can balance all optimization objectives should exist.

B. *RVEA and PARVEA*

RVEA[25]decomposes original optimization problems into different subproblems by generating adaptive reference vectors. The angle-penalized distance (APD) is employed to balance between diversity and convergence in high-dimensional space. The proposed algorithm PARVEA is based on RVEA.

The result of RVEA shows that it is superior to other algorithms in dealing with problems in higher dimensional space with many objective functions. In practical terms, RVEA has also achieved a better result in esterification process. However, RVEA has deficiencies in some respects. For example, although parameter fr can control the frequency of employing reference vectors to ensure convergence and diversity of solutions obtained in iteration process, it is a constant which may miss the best opportunity to update reference vectors. That is to say, when the value of fr is set to 50, the reference vectors will be updated every 50 iterations. In fact, for some problems, starting from the 40th iteration, for example, the distribution of the solutions may already become similar. This indicates that we should choose to update the reference vector in an earlier iteration, such as 41 instead of iteration 50 in this example. This will not only reduce the computation time, but also enable us to search more solutions in a larger space. Therefore, the RVEA algorithm loses its adaptability.

To solve this problem, a comparison of the distribution of solutions between current generation and next generation in the

optimization process is necessary by calculating Pearson correlation coefficient. Specifically, the Hadamard product is used when the number of current solutions is the same as that of next generation. As it is known, every reference vector replaces the proportion of different sub problems in objective functions. Inspired by the nature of the reference vectors, the solution should associate the Hadamard product with the corresponding vector. The detail process description is shown in Algorithm 1.

Algorithm 1: The distribution of solution

1**: Input:** generation index t; current population set $P_t = \{p_{t,1}, p_{t,2} \ldots, p_{t,m}\}$, the next population set$P_{t+1} = \{p_{t+1,1}, p_{t+1,2} \ldots, p_{t+1,n}\}$; current unit reference vector set $V_t = \{v_{t,1}, v_{t,2} \ldots, v_{t,N}\}$ the next unit reference vector set $V_t = \{v_{t+1,1}, v_{t+1,2} \ldots, v_{t+1,N}\}$; the reference vector, which current population associates with, is denoted as matrix B ; the reference vector, which next population associates with, is denoted as matrix P_6

2： **Output**：reference vector set V_{t+2}

3： m← the number of current population

4： n ← the number of next population

5：**While** m==n do

6： c ←temp.objs*V(B) % .*replaces Hadamard product

7： d ←Population2.objs*V(P_6)

8：Calculate the sum of the matrices c and d in terms of columns

9：Calculate the Pearson correlation coefficient q between C and D

10： **if** $q \geq 0.98$ **do** update the reference vector

11： **break; end**

12： **break ; end**

In Algorithm 1, m is the number of solutions in the t th iteration, and n is the number of solutions in the $t-1$ th iteration. In summary, when the value of m is equal to n, we make a Hadamard product between solutions and the reference vector which is associated with the solutions. The matrixes obtained are respectively denoted as c and d. Then we calculate the column sum of the matrices c and d, and the matrixes C and D will be respectively obtained. Last, we calculate the Pearson correlation coefficient between C and D.

When the value of Pearson correlation coefficient is more than 0.98, it indicates that the distribution of current and past moment is the same. Thus, we can update the reference vectors. If not, we will not update the reference vectors. The value of 0.98 is selected because it yields the optimal experiment results in esterification process. Through the method in Algorithm 1, the adaptability of RVEA algorithm can be increased.

The key point of RVEA algorithm is its scalarization approach, termed APD, which indicates that convergence and diversity of solutions are considered in all iteration process.

Specifically,

$$f'_{t,i} = f_{t,i} - z_t^{min} \tag{16}$$

$$d_{t,i,j} = \left(1 + M \cdot \left(\frac{t}{t_{max}}\right)^{\alpha} \frac{\theta_{t,i,j}}{\gamma_{v_{t,j}}}\right) \left\|f'_{t,i}\right\| \tag{17}$$

$$r_{v_{t,i,j}} = \frac{f'_{t,i} \cdot v_{t,j}}{\left\|f'_{t,i}\right\|} \quad \gamma_{v_{t,i,j}} = \min_{i,j=1,2.....N, i \neq j} \arg cos \left\langle v_{t,i}, v_{t,j} \right\rangle \tag{18}$$

As recommended in [25], M and N denote the number of objectives and reference vectors. Respectively $v_{t,i}$ and $v_{t,j}$, is the ith and the jth reference vector, and t replaces current number of iterations. t_{max} is the maximum number of iterations which will be defined before employing RVEA algorithm. Then $\gamma_{v_{t,j}}$replaces the smallest angle value formed by reference vector $v_{t,j}$ and other reference vectors in the current iteration, and α is a predefined parameter which is set to 2 to control the frequency of convergence.$\left\|f'_{t,i}\right\|$is the Euclidean distance calculated by population and ideal point. Specially, at the early stage of the search process (i.e.,$t \ll t_{max}$), $M \cdot \left(\frac{t}{t_{max}}\right)^{\alpha} \frac{\theta_{t,i,j}}{\gamma_{v_{t,j}}} \approx 0$ and thus $d_{t,i,j} \approx \left\|f'_{t,i}\right\|$ can be satisfied, which means that the value of $d_{t,i,j}$is mainly determined by the convergence criterion$\left\|f'_{t,i}\right\|$; at the last stage of the search process, with the value of t approaching t_{max}, $d_{t,i,j} \approx \left(1 + M \cdot \frac{\theta_{t,i,j}}{\gamma_{v_{t,j}}}\right) \left\|f'_{t,i}\right\|$,the algorithm not only concentrates on the diversity but also on the convergence, where $\theta_{t,i,j}$ represents the angle between objective vector $f'_{t,i}$ and reference vector $v_{t,j}$. Then the following improved methods are proposed.

$$d_{t,i,j} = \left(1 + \sqrt{M} \cdot \left(\frac{t}{t_{max}}\right)^{\alpha} \frac{\theta_{t,i,j}}{\gamma_{v_{t,j}}}\right) \left\|f'_{t,i}\right\| + \sqrt{M} \cdot \left(\frac{t}{t_{max}}\right)^{\alpha} \left\|f'_{t,i}\right\| cos\, \theta_{t,i,j} \tag{19}$$

The selection of the best solution through improved APD method is to find the solution on each reference vector that is the closest to the ideal point. In PARVEA, the projection distance $\left\|f'_{t,i}\right\| cos\, \theta_{t,i,j}$ and the corresponding angles $\theta_{t,i,j}$ are incorporated to balance between the convergence and diversity. Additionally, M is changed to $\sqrt{M}$ to reduce the effect of dimensions on the objective function. All of what we have done is to strengthen the convergence and diversity in the last stage of the search process.

The principle of improvement in Eq.(19) for PARVEA is displayed in Fig.2. This is an example in two-dimension space. Specially, o represents the ideal point. f_1 represents the first objective function. Similarly, f_2 is the second objective function. f' denotes the vector of population minus ideal point as shown in Eq.(16). d_1 represents the Euclidean distance of each population member from each of the reference lines in original RVEA, and d_2 represents the added projection distance of each population member from each of the reference lines in PARVEA. The core idea of Eq.(19) is that small $\theta_{t,i,j}$ does not imply these solutions are closer to the ideal point. Aiming at resolving this problem, projection distances of the solution vectors onto the associated reference vectors are considered.

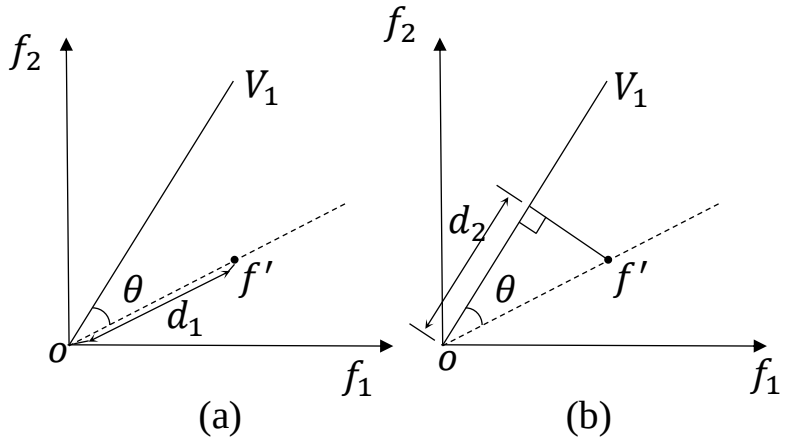

Fig. 2. (a) d_1 represents the Euclidean distance of each population member from each of the reference lines in original RVEA. (b) d_2 represents the added projection distance of each population member from each of the reference lines in PARVEA.

The reason for adding $\left(\frac{t}{t_{max}}\right)^{\alpha}$ is that the improvement of the projection distance can play adaptively an increasing role with the increased iterations. The details of PARVEA applied in the esterification process are described as follows:

Step 1: Initialization:

Step 1.1: Generate an initial population P with size N according to the constraints of the problem.

Step 1.2: Initialize N uniformly distributed reference vectors V by Das and Dennis's systematic approach[26].

Step 2: Reproduction: generate offspring population Q with size N by using binary crossover and polynomial mutation on parent population P.

Step 3: Combine parent and offspring population P=P ∪ Q.

Step 4: Associate each individual in P with a reference vector that has the smallest angle with itself.

Step 5: For each vector that has at least one individual associated with it, calculate the improved APD of every individual associate with it by Eq. (19) and select the one with the minimum improved APD. All selected individuals constitute the population Ps.

Step 6: Determine if the reference vectors need to be updated by Algorithm 1. If an update is required, update the reference vectors:

Step 6.1: Calculate the minimal and maximal objective values z_{min} and z_{max}, respectively.

Step 6.2: For each reference vector V_i, calculate the new reference vector V_i' by $V_i' = V_i \cdot (z_{max} - z_{min}) / \|V_i \cdot (z_{max} - z_{min})\|$.

Step 7: Stopping Criteria: If stopping criteria is satisfied, then stop and output P=Ps. Otherwise, go to Step 2.

Step 8: The best operating conditions of esterification process are selected by the user's preference.

IV. Performance Evaluation

A. *Evaluation Results on Esterification Process*

Four decision variables are used for optimization of the esterification process. These are the reactor pressure P(mmHg),

temperature T (iso-thermal), and residence time $\tau(min)$ of the polymeric reaction mass inside the reactor and the ratio r (the unit is 1) of slurry EG/PTA. Then the objectives are the esterification rate $E_s(\%)$, the percentage of diethylene glycol $W_t(\%)$, the average molecular mass M_n(the unit is 1) and the degree of polymerization P_n(the unit is 1). The solution of the multi-objective optimization problem described in Eq. (12) is obtained using PARVEA and RVEA with same process parameters and initial concentration of each substance as that of paper[5].

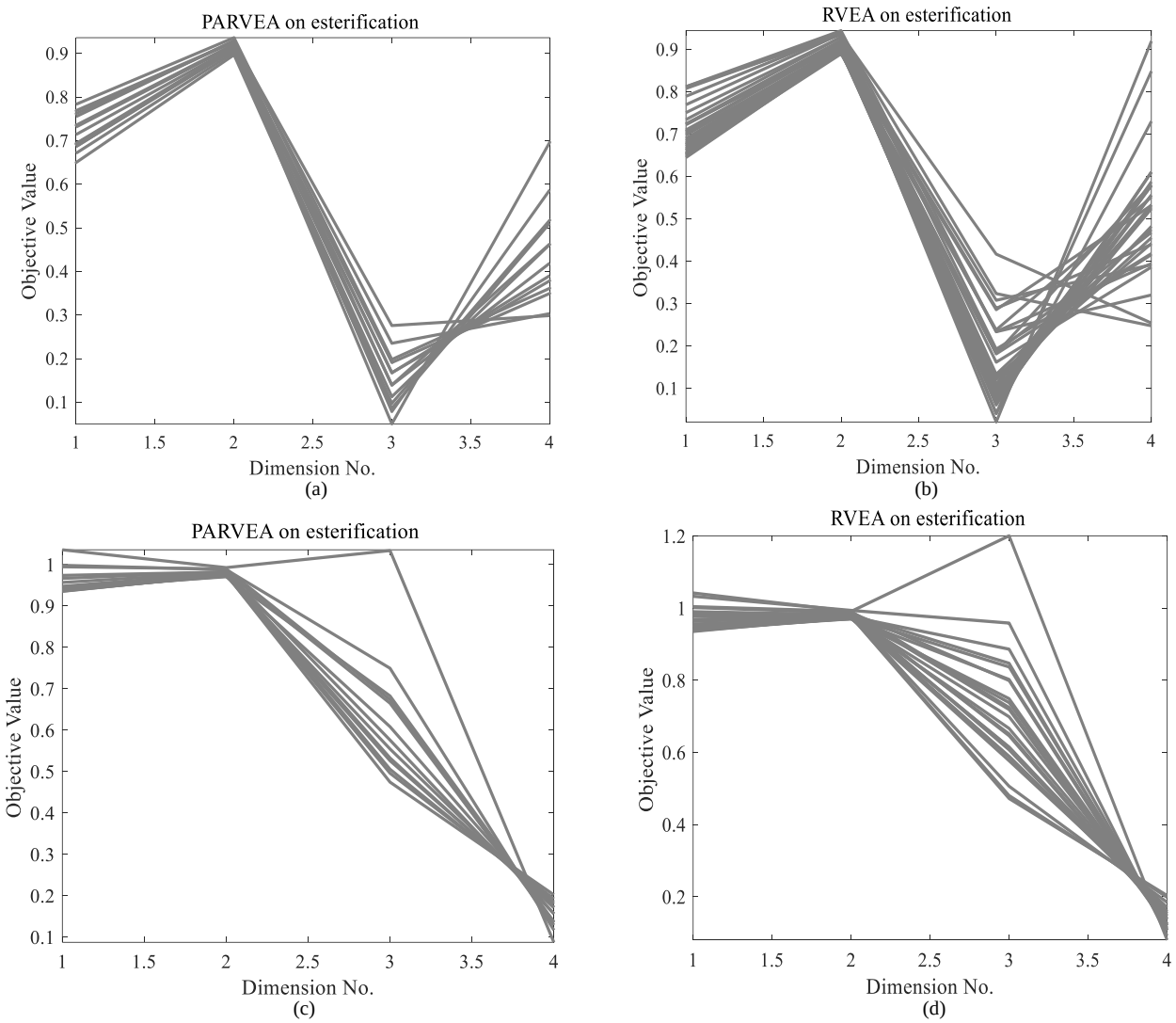

Fig. 3. Optimization results of drawing process obtained after and before improving the first principle model by PARVEA and RVEA

This is a minimization four-objective optimization problem with an unknown Pareto front. In Fig. 3, x-axis represents four different objectives. Because we want to maximize M_n, P_n and E_s. The first objective is reformulated as $1/M_n$; the second objective is reformulated as $1/P_n$; the third objective is reformulated as $1/E_s$. The fourth objective is the percentage of diethylene glycol W_t. The ordinate represents different results of four objective functions. We can see if the temperature is kept in the range from 275 to 285 degree centigrade, pressure at about standard atmosphere, the operating variables in reasonable limits, and the ratio of slurry set at about 1.1, using the improved model, then according to Fig. 3 (a) and (b), the maximized esterification rate can reach

about 95%, the average molecular mass can reach about 600, the degree of polymerization can reach about 5, and the minimized percentage of diethylene is about 0.3% to maintain the product quality. The specific range of residence time is not provided here, but it is kept in a reasonable range.

Nevertheless, from Fig. 3 (c) and (d), when the model has not been improved, that is to say, the first principle model does not consider the formation of acetaldehyde, it has lower performance than that of the improved model shown in Fig. 3(a) and (b) in esterification rate E_s, the average molecular mass M_n and the degree of polymerization P_n. Therefore, the comparison between Fig. 3 (a) (b) and (c) (d) shows that it is necessary to take the production of side reaction acetaldehyde into account in the high-dimensional and multi-objective optimization of the mechanism model of polyester fiber polymerization esterification process. The performance of RVEA and PARVEA is compared. The size of population of two algorithms is set as 100. The simulation results are shown in Fig. 3 (a) and (b). It shows also that objective function values obtained from PARVEA are smaller than those from RVEA. Especially, in terms of the first objective, the solutions obtained from PARVEA are mostly around 0.7, compared with that of RVEA which varies from 0.7 to 0.8. For the third objective, the solutions vary from 0.05 to 0.3 in PARVEA, compared with RVEA which varies from 0.05 to 0.4. The solutions of the fourth objective in PARVEA vary from 0.25 to 0.8, compared with RVEA which varies from 0.25 to 0.95.

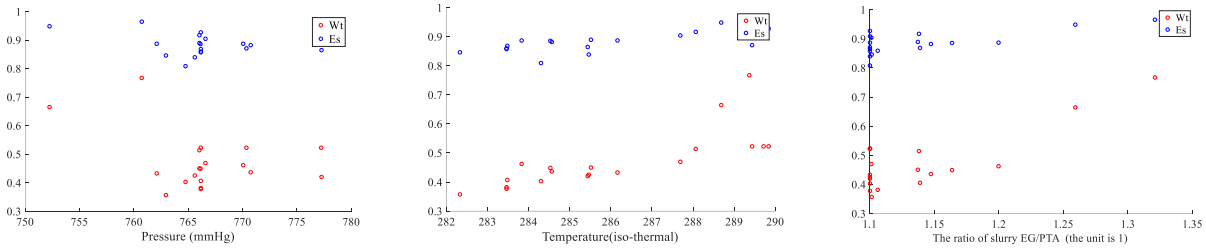

Fig. 4 Decision variables corresponding to each of the Pareto optimal solutions shown in Fig. 3 (a) (b).

Fig. 4 is a plot of the decision variables corresponding to each of the points on the Pareto set. It shows that the ratio of slurry EG/PTA is near its bound, which implies the relations between esterification rate E_s, the percentage of by-product diethylene glycol W_t and the ratio of slurry EG/PTA are approximately monotonic. Meanwhile, this phenomenon is also confirmed by the process operators, according to whom, compared with other process variable, reactor temperature and reactor pressure are most sensitive in the reaction process.

In conclusion, PARVEA can obtain solutions with smaller objective function values compared to RVEA. The IGD[27] values may heavily depend on the real Pareto set. Thus, we calculate HV[28]additionally for further comparison. The HV values obtained by RVEA and PARVEA algorithms in 20 independent runs are shown in TABLE IV. The reference point in HV is set as [1 1 1 2] which is dominated by all Pareto solutions obtained from PARVEA and RVEA. TABLE IV shows the mean and standard deviation of HV values over 20 independent runs. The Wilcoxon rank sum test is also used to compare the results at a significance level of 0.05.

Symbol '-' means the result of PARVEA is significantly better than that of RVEA.

TABLE IV
The mean and standard deviation results of HV values calculated by RVEA and PARVEA

Problem	*M*	RVEA	PARVEA
Esterification	4	1.2872e-2 (1.37e-4) -	1.3070e-2 (9.00e-5)
+/-/=		0/1/0	

Furthermore, the standard deviations are listed in parentheses in TABLE IV. One can see that the proposed algorithm not only has better convergence and diversity, but also has better stability. The stability of the solutions is what is needed in actual industrial production process. In the actual industrial production, each adjustment of the process parameters can bring large losses.

In summary, the aim of proposed PARVEA is to find the optimal operating conditions to optimize product performance in production process of polyester fiber polymerization esterification. It shows that PARVEA can choose better optimal operating conditions under the same objective function value in these simulations.

B. Experimental Settings in the Test Problems

The algorithms are implemented in MATLAB R2016a and run on a PLATEMO[29].We adopt DTLZ1-DTLZ7[30]taken from the DTLZ test suites that are widely used benchmark test problems to compare PARVEA with other algorithms of multi-objective optimization. The number of decision variables is set to n=M+K-1, where M is the number of optimization objectives. K=5 is used for DTLZ1, and K=10 is used for test problems from DTLZ2 to DTLZ7. For each test problem, objective function values varying from 4 to 10, i.e. $M \in \{4,6,8,10\}$are considered. HV and IGD are used as the performance indicators in empirical experiment comparisons between the results obtained by PARVEA and other algorithms. Because the IGD value depends on not only the number of the obtained solutions but also the true Pareto Front, the suitable IGD value can be obtained to balance the convergence. The results are shown in TABLE IV. Similarly, the HV value is used as the performance indicator to balance diversity by all Pareto-optimal solutions. The results are shown in TABLE V. Each algorithm is run for 20 times on each test problem independently.

C. IGD Results on the Test Suits

The IGD is calculated as follows:

$$IGD(B, Z_{eff}) = \frac{1}{|Z_{eff}|}\sum_{i=1}^{|Z_{eff}|} min \overset{|B|}{\underset{j=1}{d}}(z_i, b_j) \qquad (20)$$

Where $B = [b_1, b_2 \ldots]$ is the nondominated individuals obtained by an MOEA in the objective space. $Z_{eff} = [z_1, z_2, \ldots]$ is a set of solutions sampled from the known Pareto front. $d(z_i, b_j) = \|z_i - b_j\|_2$ represents the Euclidean distance from z_i to b_j. The IGD metric is able to measure both diversity and convergence of B, when the $|Z_{eff}|$ is large enough.

TABLE V
The statistical rank results (mean) of IGD values on DTLZ problems calculated by RVEA, MOEADPaS, SPEAR, DMOEAeC and PARVEA

	DTLZ1				DTLZ2				DTLZ3				DTLZ4				DTLZ5				DTLZ6				DTLZ7			
M	4	6	8	10	4	6	8	10	4	6	8	10	4	6	8	10	4	6	8	10	4	6	8	10	4	6	8	10
RVEA	**1**	2	**1**	2	2	2	2	2	**1**	**1**	**1**	2	2	2	2	2	5	3	3	3	5	2	2	2	4	3	4	3
SPEAR	5	4	4	4	4	3	3	3	4	4	4	4	4	3	3	3	4	5	5	5	4	5	5	4	2	4	3	4
MOEADPaS	4	5	5	5	5	5	5	5	5	5	5	5	5	5	5	4	3	4	4	4	2	4	3	5	5	5	5	5
DMOEAeC	2	3	3	3	3	4	4	4	2	3	3	3	3	4	4	5	2	2	2	2	3	3	4	3	3	**1**	2	2
PARVEA	3	**1**	2	**1**	**1**	**1**	**1**	**1**	3	2	2	**1**	**1**	**1**	**1**	**1**	**1**	**1**	**1**	**1**	**1**	**1**	**1**	**1**	**1**	2	**1**	**1**

TABLE VI
The statistical rank results (mean) of HV values on DTLZ problems calculated by RVEA, MOEADPaS, SPEAR, DMOEAeC and PARVEA

	DTLZ1				DTLZ2				DTLZ3				DTLZ4				DTLZ5				DTLZ6				DTLZ7			
M	4	6	8	10	4	6	8	10	4	6	8	10	4	6	8	10	4	6	8	10	4	6	8	10	4	6	8	10
RVEA	**1**	**1**	**1**	**1**	2	2	2	2	**1**	**1**	**1**	**1**	2	2	2	2	5	3	3	2	3	2	2	3	4	4	4	2
SPEAR	5	4	3	4	3	3	3	3	5	4	4	5	3	4	4	3	4	5	5	4	5	5	5	4	3	3	3	3
MOEADPaS	3	5	5	5	5	5	5	5	4	5	5	4	5	5	5	4	3	4	4	5	2	3	4	5	5	5	2	4
DMOEAeC	2	2	2	2	4	4	4	4	2	3	3	3	4	3	3	5	2	2	2	**1**	4	4	3	**1**	2	**1**	**1**	**1**
PARVEA	4	3	4	3	**1**	**1**	**1**	**1**	3	2	2	2	**1**	**1**	**1**	**1**	**1**	**1**	**1**	3	**1**	**1**	**1**	2	**1**	2	5	5

These parameter settings are the same as recommended in RVEA for test problems from DTLZ1 to DTLZ7.TABLE V presents IGD results of PARVEA, RVEA, SPEAR[31], DMOEAeC[32]and MOEADPaS[33] from 4-objective to 10-objective in test problems of from DTLZ1 to DTLZ7. The statistical results of the IGD values obtained by the five algorithms are summarized in TABLE V, where the best results are highlighted. TABLE V for 4 to 10-objective normalized DTLZ test problems shows that (i) PARVEA performs best in DTLZ2, DTLZ4, DTLZ5 and DTLZ6 test suites, and performs best in DTLZ7 on 4 to 10-objective except 6-objective in terms of IGD value. (ii) DMOEAeC algorithm performs better on 6-objective in a non-uniformly distributed Pareto-optimal front (like in the DTLZ7 problem) than other algorithms, but PARVEA performs better on other objectives than other algorithms. (iii) PARVEA approaches are overperformed by RVEA in DTLZ3 problem on 4 to 8-objective, but performs better on other objectives than other algorithms. Overall, PARVEA obtains the best results on twenty-two out of twenty-eight test instances, so it can be seen that PARVEA shows better capability in approximating true Pareto fronts compared to the state-of-the-art algorithms.

D. HV Results on the Test Suites

The hypervolume index (HV) measures the volume of the dimensional region in the target space surrounded by the non-dominating solution set and the reference point obtained by the MOEAs. The detail is shown as follows:

$$HV = \delta\left(\cup_{i=1}^{|S|} v_i\right) \tag{21}$$

where δ represents the Lebesgue measure which is used to measure volume. $|S|$ represents the number of nondominated sets. v_i represents the supercube formed by the reference point z^* and the i th solution in the solution set. Above all, it indicates, first, the larger the value of HV, the better performance the algorithm has. Second, the value of HV is determined by the reference point.

The reference points used in the HV calculation are set as $(z_1^{max} + 0.1, z_2^{max} + 0.1, \ldots . z_{\mathrm{M}}^{max} + 0.1)$, where $z_1^{max}$to $z_M^{max}$are the maximum objective values calculated from the five algorithms. Except the 10-objective problem of DTLZ5 and DTLZ6, the rest

HV values are normalized to [0, 1]. Based on the results shown in the TABLE VI on 4 to 10-objective normalized DTLZ test problems, it can be concluded that (i) RVEA performs best in DTLZ3 on 4 to 10-objective in terms of HV value. (ii) PARVEA performs best in DTLZ2, DTLZ4, DTLZ5 and DTLZ6 on 4 to 10-objective except the 10-objective on DTLZ5 and DTLZ6. (iii) Meanwhile, in a non-uniformly distributed Pareto-optimal front (like in the DTLZ7 problem), DMOEAeC performs best on 6 to 10-objective. Especially, DMOEAeC outperforms other algorithms in DTLZ5 and DTLZ6 problems on 10-objective. In summary, PARVEA obtains the best results on fifteen out of twenty-eight test instances.

V. Conclusion

To the best of our knowledge, this work is the first to obtain a four-objective optimization of the esterification process in PET polymerization through the RVEA algorithm. The PARVEA algorithm is proposed based on original RVEA algorithm. The main idea is that not only the projection distance is incorporated into the Angle-Penalized Distance, but reference vector is updated adaptively according to the distribution of the solution. Meanwhile, PARVEA is applied to optimize the esterification process. The simulation results are consistent with the operation of the factory, which indicates the effectiveness of PARVEA. In addition, the proposed PARVEA algorithm is compared with other four different algorithms on DTLZ1 to DTLZ7 test problems. The experimental results verify the effectiveness of PARVEA.

Then companies can choose more suitable solutions and process parameters obtained by PARVEA algorithm according to user preferences, which can meet the requirements for differentiated production of high-quality polyester fiber polymers.

Our future work includes improving the solutions diversity of PARVEA and extending it to solving more practical problems, such as the dynamic multi-objective optimization of polymerization process.

Acknowledgment

This work was supported in part by the National Key Research and Development Plan from Ministry of Science and Technology under Grant 2016YFB0302701, National Natural Science Foundation of China under Grant 61603090, Natural Science Foundation of Shanghai under Grant 19ZR1402300, the Fundamental Research Funds for the Central Universities under Grant 2232017D-13. in part by the Graduate Innovation Fund in Donghua University under Grant CUSF-DH-D-2020078.

References

1.Mandal S, Dey A. PET Chemistry. *Recycling of Polyethylene Terephthalate Bottles*, 2019:1-22.

2.Islam MT, Rahman. Polymers for Textile Production. *Frontiers of Textile Materials*, 2020:13-59.

3.Y. Hu, Mathematical Model of Direct Esterification Process of Polyester, *Beijing University of Chemical Technology*, 2003.

4.Yao Z, Ray WH. Modeling and analysis of new processes for polyester and nylon production. *AIChE Journal*, 2001;47(2):401-412.

5. Bhaskar V, Gupta SK, Ray AK. Multiobjective optimization of an industrial wiped-film pet reactor. *AIChE Journal*, 2000;46(5):1046-1058.

6.Y. Zheng, W. Fan, and W. Zhang, Study on the Uniformity of Polyester Reaction, *Polyester Industry*, 2002, vol. 15, no. 4, pp. 8-11.

7. Luo N, Qian F. Parameter estimation of industrial PET reactor using multi-objective kernel density estimation of distribution algorithm. *Asia-Pacific Journal of Chemical Engineering*, 2012;7(5):783-794.

8.Liu T, Gu X, Wang J, Feng L, Intensification P-P. Modeling and analysis of new reactor concepts for poly (ethylene terephthalate) esterification process. *Chemical Engineering and Processing-Process Intensification*, 2019;135:217-226.

9.S. Wu. Process Simulation of Polyester Systems [D]. *Beijing University of Chemical Technology*, 2009.

10.Kumar PS, Joshiba GJ. Properties of Recycled Polyester. *Recycled Polyester: Springer*; 2020:1-14.

11.W. Shi, Optimization of Esterification Process Based on Multi-objective Genetic Algorithm, 2003.

12.Cao L, Wang J, Jiang P, Jin Q. Multiobjective intelligence optimal operation of PET polymerization. Paper presented at: *2011 9th World Congress on Intelligent Control and Automation2011*.

13.Peng W,. High-Dimensional Multi-Objective Optimization Strategy Based on Decision Space Oriented Search. *Cloud and Service-Oriented Computing*, 2019;1(1):1-6.

14.Bhat SA, Huang B. Preferential crystallization: Multi-objective optimization framework. *AIChE Journal*, 2009;55(2):383-395.

15.Panda D, Ramteke. Preventive crude oil scheduling under demand uncertainty using structure adapted genetic algorithm. *Applied Energy*, 2019;235:68-82.

16.Cao X, Jia S, Luo Y, Yuan X, Qi Z, Yu K. Multi-objective optimization method for enhancing chemical reaction process. *Chemical Engineering Science*, 2019;195:494-506.

17.Zitzewitz P, Fieg G. Multi-objective optimization superimposed model-based process design of an enzymatic hydrolysis process. *AIChE Journal*, 2017;63(6):1974-1988.

18.Parhi SS, Rangaiah GP, Jana AK. Multi-objective optimization of vapor recompressed distillation column in batch processing: Improving energy and cost savings. *Applied Thermal Engineering*, 2019;150:1273-1296.

19.del Rio-Chanona EA, Wagner JL, Ali H, Fiorelli F, Zhang D, Hellgardt. Deep learning-based surrogate modeling and optimization for microalgal biofuel production and photobioreactor design. *AIChE Journal*, 2019;65(3):915-923.

20.Zhang Q, Li H. MOEA/D: A multiobjective evolutionary algorithm based on decomposition. *IEEE Transactions on Evolutionary Computation*, 2007;11(6):712-731.

21.Cheng R, Rodemann T, Fischer M, Olhofer M, Jin Y. Evolutionary many-objective optimization of hybrid electric vehicle control: From general optimization to preference articulation. *IEEE Transactions on Emerging Topics in Computational Intelligence*, 2017;1(2):97-111.

22.Zhu X, Hao K, Tang X, Wang T, Hua Y, Liu X. The multi-objective optimization of esterification process based on improved NSGA-III algorithm. Paper presented at*: 2019 12th Asian Control Conference (ASCC)2019*.

23.Yamada T, Imamura Y, Engineering. Simulation of continuous direct esterification process between terephthalic acid and ethylene glycol. *Polymer-Plastics Technology and Engineering*, 1989;28(7-8):811-876.

24.Xie R, Hao K, Huang B, Chen L, Cai X. Data-driven modeling based on two-stream λ gated recurrent unit network with soft sensor application. *IEEE Transactions on Industrial Electronics*. 2019:1-1.

25.Cheng R, Jin Y, Olhofer M, Sendhoff B. A Reference Vector Guided Evolutionary Algorithm for Many-Objective Optimization. *IEEE Transactions on Evolutionary Computation*. 2016;20(5):773-791.

26. Das I, Dennis. Normal-boundary intersection: A new method for generating the Pareto surface in nonlinear multicriteria optimization problems. *SIAM journal on optimization*,1998;8(3):631-657.

27.Hua Y, Jin Y, Hao K. A clustering-based adaptive evolutionary algorithm for multiobjective optimization with irregular pareto fronts. *IEEE Transactions on Cybernetics*, 2018;49(7):2758-2770.

28.Ishibuchi H, Imada R, Setoguchi Y, Nojima Y. Reference point specification in hypervolume calculation for fair comparison and efficient search. Paper presented at: *Proceedings of the Genetic and Evolutionary Computation Conference2017*.

29.Tian Y, Cheng R, Zhang X, Jin Y. PlatEMO: A MATLAB Platform for Evolutionary Multi-Objective Optimization [Educational Forum]. *IEEE Computational*

Intelligence Magazine. 2017;12(4):73-87.

30. Deb K, Thiele L, Laumanns M, Zitzler E. Scalable test problems for evolutionary multiobjective optimization. *Evolutionary multiobjective optimization: Springer*; 2005:105-145.

31. Jiang S, Yang S. A strength Pareto evolutionary algorithm based on reference direction for multiobjective and many-objective optimization. *IEEE Transactions on Evolutionary Computation*, 2017;21(3):329-346.

32. Chen J, Li J, Xin B. DMOEA-$\varepsilon\text {C} $: Decomposition-Based Multiobjective Evolutionary Algorithm With the $\varepsilon $-Constraint Framework. *IEEE Transactions on Evolutionary Computation*, 2017;21(5):714-730.

33. Wang R, Zhang Q, Zhang T. Decomposition-based algorithms using Pareto adaptive scalarizing methods. *IEEE Transactions on Evolutionary Computation*, 2016;20(6):821-837.